Ghost transmission: How large basis sets can make electron transport calculations worse

Carmen Herrmann,[1,a)] Gemma C. Solomon,[1] Joseph E. Subotnik,[1] Vladimiro Mujica,[1,2] and Mark A. Ratner[1]

[1]*Department of Chemistry, Northwestern University, 2145 Sheridan Road, Evanston, Illinois 60208-3113, USA*

[2]*Center for Nanoscale Materials, Argonne National Laboratory, Argonne, Illinois 60439, USA and Department of Chemistry and Biochemistry, Arizona State University, Tempe, Arizona 85287, USA*

(Received 26 October 2009; accepted 11 December 2009; published online 12 January 2010)

The Landauer approach has proven to be an invaluable tool for calculating the electron transport properties of single molecules, especially when combined with a nonequilibrium Green's function approach and Kohn–Sham density functional theory. However, when using large nonorthogonal atom-centered basis sets, such as those common in quantum chemistry, one can find erroneous results if the Landauer approach is applied blindly. In fact, basis sets of triple-zeta quality or higher sometimes result in an artificially high transmission and possibly even qualitatively wrong conclusions regarding chemical trends. In these cases, transport persists when molecular atoms are replaced by basis functions alone ("ghost atoms"). The occurrence of such ghost transmission is correlated with low-energy virtual molecular orbitals of the central subsystem and may be interpreted as a biased and thus inaccurate description of vacuum transmission. An approximate practical correction scheme is to calculate the ghost transmission and subtract it from the full transmission. As a further consequence of this study, it is recommended that sensitive molecules be used for parameter studies, in particular those whose transmission functions show antiresonance features such as benzene-based systems connected to the electrodes in *meta* positions and other low-conducting systems such as alkanes and silanes. © *2010 American Institute of Physics*. [doi:10.1063/1.3283062]

I. INTRODUCTION

From early work in the late 1940s[1] and the first proposal of a single-molecule device in 1974,[2] the field of molecular electronics has grown into a very active area of research. "Molecular electronics" may be defined as the study of electronic circuits containing individual molecules as building blocks.[3–19] The most prominent example of such a circuit is a molecular transport junction, where one molecule is sandwiched between two macroscopic electrodes. In a typical experiment, the electron current I through this device is measured as a function of bias voltage V (I-V curve) and often also as a function of gate voltage. The "molecular" characteristics of the junction are revealed particularly in deviations from Ohmic behavior, i.e., in nonlinear I-V curves.

A strong motivation for theoretical calculations of molecular conduction is that they may provide further insight into the mechanisms of electron transport, often interpreted in terms of auxiliary, nonmeasurable quantities such as molecular orbitals (MOs), and therefore may help to design new types of molecular devices.[20–23] Apart from this practical importance for interpreting and designing experiments, the theoretical description of current through molecules is equally appealing from a purely scientific (rather than technological) point of view: a satisfying description of the process requires knowledge of electronic structure theory for stationary states,[24] electron dynamics,[25] and the physics of open systems away from equilibrium.[26,27] There is also a strong connection to various other fields of research, in particular, a formal analogy may be made[28–30] between electron transport through molecular junctions and intramolecular electron transfer (ET) in donor-bridge-acceptor systems.[31–34]

Ideally, theory-based predictions should not rely on any system-specific input data and be sufficiently accurate for the desired purpose. In principle, this combination is achieved by methods based on first-principles quantum mechanics, using natural constants as the only input quantities obtained from experiment. For devices of practical interest, however, the resulting equations of motion are very far from being solvable—one very obvious reason is that a straightforward application of quantum mechanics would require describing macroscopic electrodes on the same footing as the single molecule placed between them. Therefore, several approximations have to be made in practice, and the errors thus introduced are often poorly understood.

Altogether, the theory of electron transport is in a rather early stage of development compared with more established areas of research such as molecular electronic structure theory,[24] vibrational spectroscopy,[35,36] or molecular dynamics.[37,38] This may be ascribed to the complex nature of an open system under nonequilibrium conditions. Nonetheless, in recent years, one set of approximations has evolved

[a)]Author to whom correspondence should be addressed. Electronic mail: c-herrmann@northwestern.edu. FAX: +1-847-467-4996. Tel.: +1-847-467-4984.

into what may be regarded as the "standard approach" to first-principles calculations in molecular electronics, and has been shown to give a reasonable agreement with experimental results.[39] This is the combination of the Landauer–Imry elastic scattering treatment[40–42] with a nonequilibrium Green's function (NEGF) approach[27,43] and Kohn–Sham density functional theory (KS-DFT),[44,45] or other electronic-structure descriptions which give a simple MO picture, such as Hartree–Fock (HF) theory, tight-binding approaches,[46] or extended Hückel theory. Recently, the Landauer–Imry approach has also been combined with Møller–Plesset perturbation theory.[47]

The limitations of the Landauer approximation, such as its effective single-particle nature, and its restriction to coherent electron transport processes are well-known. Although considerable progress has been made in the recent years, it still remains a challenge, even for very sophisticated implementations of the Landauer approximation (such as those described, e.g., in Refs. 48–51), to predict the order of magnitude of the measured zero-voltage conductance correctly. Undoubtedly, this is in part due to the unknown contact structure. It also appears that more elaborate approaches do not necessarily perform better than less sophisticated ones.[39] It is therefore hard to establish the extent to which the approximations made in these transport approaches limit the accuracy of the method. Our goal in this paper is to ensure that at a minimum, no additional errors are introduced by the choice of technical settings in the electronic structure calculation, such as the atom-centered basis set in a KS-DFT calculation. This benchmarking will be particularly important for molecules with a complicated electronic structure, such as transition metal complexes and other open-shell systems.

Several parameter studies within the Landauer approach have been published, focusing on the influence of the density functional,[52–55] the basis set,[53,54,56] and the number of electrode atoms included in the electronic-structure calculation.[54,57–59] Reference 56 is the first example of a basis set study including basis sets of triple-zeta quality and polarization functions. In contrast to Ref. 60, which considers a double-zeta basis set with polarization functions as sufficient, Ref. 56 points out that to achieve convergence with respect to the basis set size, a basis set of at least triple-zeta quality is necessary. This coincides with experience from isolated-molecule studies, which suggest that a double-zeta basis set may be far from adequate.[61]

In Refs. 56 and 60, molecules based on *para*-connected phenyl rings are chosen as test systems, In this work, we show that when studying molecules with lower conductance and more structure-sensitive transport properties, such as *meta*-connected phenyl-based molecules, and when employing large atom-centered, nonorthogonal basis sets of Slater or Gaussian type (as commonly used in quantum chemistry), a large basis set may lead to artificially high transmission. This high transmission is also observed when the molecule's atoms are replaced by ghost atoms (i.e., basis functions only), a result that we here call "ghost transmission." This may be related to other accounts of situations where employing a larger basis set does not necessarily lead to more accurate results, in particular when calculating nonvariational properties, but also for dimerization energies.[62]

This manuscript is organized as follows. First, the implementation of the Landauer approximation employed here is briefly outlined, and the concept of ghost transmission is introduced. In Sec. III ghost transmission is shown to be of practical concern for predicting the qualitative difference in transmission between alkanes in two different conformations. The causes of ghost transmission are investigated in detail for a small model junction (Sec. IV). The insight gained so far is applied in Sec. V to a *meta*-connected benzene junction. Finally, in Sec. VI, the nature of the virtual MOs causing ghost transmission is discussed. Additional information on the implications of large basis sets on the approximate description of the bulk electrodes in the wide-band-limit (WBL) approximation, as well as details on the computational methodology, can be found in the appendices. The supplementary material[63] provides data on the importance of different molecular regions for ghost transmission, ghost transmission at the basis set limit, the effect of exact exchange admixture in the exchange-correlation functional and the distance between the electrodes, and the change in partial charges with the basis sets employed here as well as the importance of interelectrode coupling.

II. THEORY AND ALGORITHMIC DETAILS

The combination of Landauer–Imry approach and NEGF formalism employed here for calculating currents through a quantum system is based on the following assumptions and approximations.

- The system is described within an effective one-particle approach such as HF theory or KS-DFT.
- The coupling between the quantum system and the electrodes is large enough to prevent substantial accumulation of charge (which would be considered the Coulomb blockade regime).
- The electrodes are reflectionless, i.e., there is no backscattering once a charge has passed the central region-electrode interface.
- The transport is coherent, i.e., no phase breaking events occur. This is usually a good assumption when dealing with short molecular bridges, low temperatures, and a large separation between the one-particle energy levels and the Fermi energies of the electrodes.
- The system is in a steady state, i.e., the number of electrons in the central region is constant over time.
- The entire electrode-central region-electrode system is described by a basis whose elements can be clearly attributed to either electrode or the central region.

The original Landauer equation relates the zero-temperature, zero-voltage conductance of a quantum system to the value of a transmission function at the Fermi energy,[40–42] without giving a detailed prescription of how to deal with particular bridges. This was achieved by the introduction of techniques to calculate the transmission function

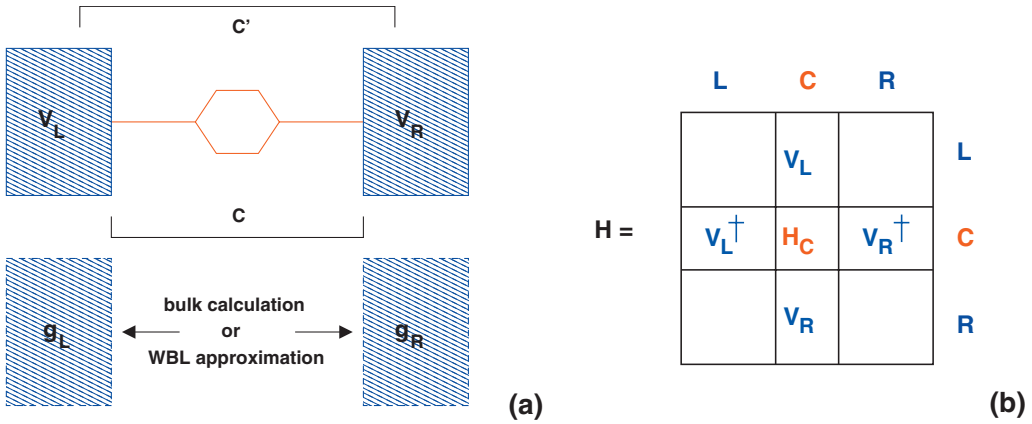

FIG. 1. (a) Partitioning of the full electrode-molecule-electrode system as employed in a finite cluster approach. Two alternative definitions of the central system are shown, one that only comprises the molecule (C), and one that comprises the molecule and several electrode atoms (C'). (b) Definition of the central subsystem Hamiltonian and the coupling matrices as submatrices of the full one-particle Hamiltonian.

based on a set of local orthogonal basis functions, employing Keldysh's perturbation theory for nonequilibrium systems (i.e., a NEGF approach).[64–66] It was obviously desirable to combine this transport formalism and the experience gained with molecular electronic structure calculations using *nonorthogonal* atom-centered Gaussian- or Slater-type basis sets,[67] and such implementations have become available in the past decade.[49,50,68–78] For an approach to calculating ET matrix elements in a nonorthogonal basis, see Ref. 79. Since the derivations of the equations to be implemented have been discussed extensively in the literature references cited above, they shall only be briefly summarized here.

A. The Landauer approach in a nonorthogonal basis

The current I_s of electrons of spin s ($s \in \{\alpha,\beta\}$) through the molecular junction at a given bias voltage V is calculated as

$$I_s(V) = \frac{e}{h}\int_{-\infty}^{\infty} dE T_s(E,V)[f(E-E_{F,s}^L) - f(E-E_{F,s}^R)], \quad (1)$$

where the transmission function T_s for electrons of energy E is given as

$$T_s(E,V) = \mathrm{tr}(\mathbf{\Gamma}_{R,s}\mathbf{G}_{C,s}\mathbf{\Gamma}_{L,s}\mathbf{G}_{C,s}^{\dagger}), \quad (2)$$

and f denotes the Fermi function. The appropriate definition of the Fermi energy $E_{F,s}^X$ for electrons of spin s in electrode X is an issue under discussion in the literature ("band lineup problem"[80]). One possible answer might be that if a molecule is attached to sufficiently large finite metal clusters (such as the about 500 atoms discussed in Ref. 50; compare also Ref. 81), the Fermi energy of the electrodes can be estimated as the energy halfway between the highest-energy occupied molecular orbital (HOMO) and the lowest-energy unoccupied molecular orbital (LUMO) of the metal cluster.[50] Another approach is to solve the Poisson equation for the entire system; this gives $E_{F,s}^X$ directly.[82]

The coupling matrices for the left and the right electrodes, $\mathbf{\Gamma}_{X,s}(X \in \{R,L\})$, are calculated from the imaginary parts of the corresponding self-energies $\mathbf{\Sigma}_{X,s}$,

$$\mathbf{\Gamma}_{X,s} = i(\mathbf{\Sigma}_{X,s} - \mathbf{\Sigma}_{X,s}^{\dagger}) = -2\ \mathrm{Im}(\mathbf{\Sigma}_{X,s}), \quad (3)$$

which in turn may be obtained as

$$\mathbf{\Sigma}_{X,s} = (E\mathbf{S}_{XC} - \mathbf{V}_{X,s})^{\dagger}\mathbf{g}_{X,s}(E\mathbf{S}_{XC} - \mathbf{V}_{X,s}), \quad (4)$$

where $\mathbf{g}_{X,s}$ is the retarded Green's function of the isolated electrode X [see Eq. (6) below for details]. $\mathbf{S}_X$ and $\mathbf{V}_X$ are the overlap matrix and the one-particle Hamiltonian (or Fock) matrix involving electrode X and central system basis functions (see Fig. 1).

The central subblock of the retarded Green's function is calculated as

$$\mathbf{G}_{s,C} = (E\mathbf{S}_C - \mathbf{H}_C - \mathbf{\Sigma}_R - \mathbf{\Sigma}_L)^{-1}, \quad (5)$$

where $\mathbf{S}_C$ and $\mathbf{H}_C$ are the central subblocks of the overlap and one-particle Hamiltonian matrices.

B. Details of the implementation

After neglecting effects such as molecular vibrations and external fields, electron transport through a molecular bridge is determined by three factors: the geometric and electronic structure of the molecule, the geometric and electronic structure of the electrodes, and the coupling between electrodes and molecule. The goal of our approach is to describe the contribution the molecule makes to the transport properties, irrespective of the measurement environment. That is, to identify and compare the transport properties of different molecules regardless of the electrode material, the details of their binding to the electrodes, and the question of whether they are investigated in a transport junction, in a scanning tunneling microscope (STM) setup, or an ET experiment. Among the many ways to carry out such comparative studies, we choose one that gives a reasonably good description of a very popular way of measuring transport properties, a molecular junction employing gold electrodes.

The Green's functions of the electrodes are calculated in the WBL approximation,[83]

$$(\mathbf{g}_X)_{ij} = -i\cdot\pi\cdot \mathrm{LDOS}^{\mathrm{const}}\cdot\delta_{ij}, \quad (6)$$

assuming a local density of states (LDOS) which is independent of the energy, and which in our case is chosen equal to

the LDOS of the 6*s* band as calculated for gold.[84] Our implementation is based on a finite-cluster approach, i.e., the molecule is attached to two finite clusters of metal atoms on each side (see Fig. 1), and no periodic boundary conditions are enforced.

For all calculations reported here, we use approach C in Fig. 1 with Au_9 clusters mimicking the coupling to a Au(111) surface according to Eq. (4), and with the Green's functions of the bulk electrodes described by Eq. (6) (see Appendix C for details).

Testing the basis set limit using more sophisticated descriptions of the transport—for example, the gold cluster sizes of up to 500 atoms as used in Ref. 50—would make such a study almost prohibitive within the computational resources available today. It may be anticipated, however, that the main basis set effects can be observed regardless of which model is used to describe the open-boundary conditions of a molecular junction, which is why we focus on a simple implementation of the WBL approximation in this work.

The only quantities needed from an electronic structure code are therefore the overlap matrix **S** and the one-particle Hamiltonian matrix (i.e., the Fock matrix) **H** for a molecule coupled to a finite number of electrode atoms on two sides. Since our focus is on the molecule, the central region of our setup contains either the molecule only or the molecule and a few electrode atoms. This causes problems with the band lineup,[50] but may be considered an acceptable trade-off for having the transmission properties of the molecule filtered out. The coupling matrices $V_{R,L}$ in Eq. (4) are the elements of the Fock matrix in the central region-electrode blocks. Furthermore, the open nature of the system and the effect of any bias voltage are not taken into account in the electronic structure calculations, i.e., the density matrix in the self-consistent field (SCF) algorithm is calculated, as usual in electronic structure theory of closed systems, from the MO coefficients, and not from the central subsystem block of the lesser Green's function as often done for open systems.[48,49,75] This allows a transport code to be constructed as a postprocessing tool for electronic structure calculations. That is, our transport calculations consist of two steps: (1) electronic structure calculation and (2) calculation of transmission function and, if desired, current and conductance.

C. Ghost transmission

In this work, two types of transport calculations are carried out, denoted as "full" and "ghost." A full transport calculation corresponds to the regular approach described above, where a molecule is put between two metal clusters and the transmission (and current) are subsequently calculated. In a ghost transport calculation, the same metal-molecule-metal junction is considered, but all atomic nuclei and electrons associated with atoms in the central region are removed in the electronic structure calculation, so that all that remains are the basis functions centered on these atoms (see Fig. 2).

This corresponds to the ghost basis employed in the counterpoise correction scheme for the basis set superposition error.[85] It should be noted that depending on the number of atoms in the electrode, these ghost transmission calculations may have to be carried out in a different spin state from the full ones—for example, when employing Au_9 clusters as done here, the full calculations were carried out with no unpaired electrons, while the ghost transmission was calculated having two unpaired electrons (one on each gold cluster). For the remainder of this paper, the ghost transmission curves will always be reported for spin up electrons, because only minor differences were obtained for the spin down electrons. Convergence of the SCF algorithm has been found to be difficult in some cases, but the resulting ghost transmission curves were not affected to any significant extent by convergence issues.

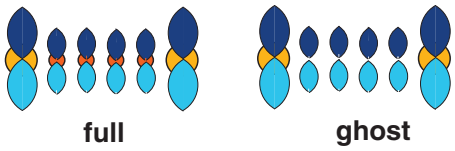

FIG. 2. Schematic illustration of the ghost basis setup for a model junction consisting of a Au–H–H–H–H–Au chain, where the central region is defined as the four H atoms. While a full calculation (left) contains both the basis functions (for simplicity, only one *p* function per atom is shown, denoted by the blue lobes) and the atomic nuclei with all electrons associated with the neutral atoms (denoted by golden and red circles), the ghost calculation (right) has the atomic nuclei and the electrons removed in the central region.

As detailed below, we will show that the transmission curves of transport calculations using large atom-centered basis sets may be interpreted approximately as the sum of a molecular transmission and the ghost transmission. We therefore consider the ghost transmission as significant when it is large enough that when subtracted from the full transmission, the shape of the transmission curve changes substantively.

III. GHOST TRANSMISSION IN ALKANE AND SILANE JUNCTIONS

A striking example of the ghost transmission problem is the comparison of transport calculations for octanedithiolate in two different conformations, one with all carbon centers in an *anti* conformation, and one with two of them in a *syn* conformation to form a local U-shaped structure (see left panel of Fig. 3).

Whereas a calculation using the double-zeta quality basis set LANL2DZ gives the qualitative prediction that the transmission function of the all-*anti* conformation is higher than the *syn* one at all energies considered, the transmission is predicted to be about the same for both conformations when employing the triple-zeta basis set with polarization functions TZVP for all energies above −5.5 eV, a range which encompasses all common choices for the Fermi energy within a KS-DFT approach.

When calculating the transmission using the ghost basis setup described in Sec. II C, significant values can be obtained, despite the fact that no molecule is present in the junction. The ghost transmission is nearly constant over the energy range considered, and it is about the same for both conformations. The similarity in the transmission curves obtained from the full and the ghost basis TZVP calculations

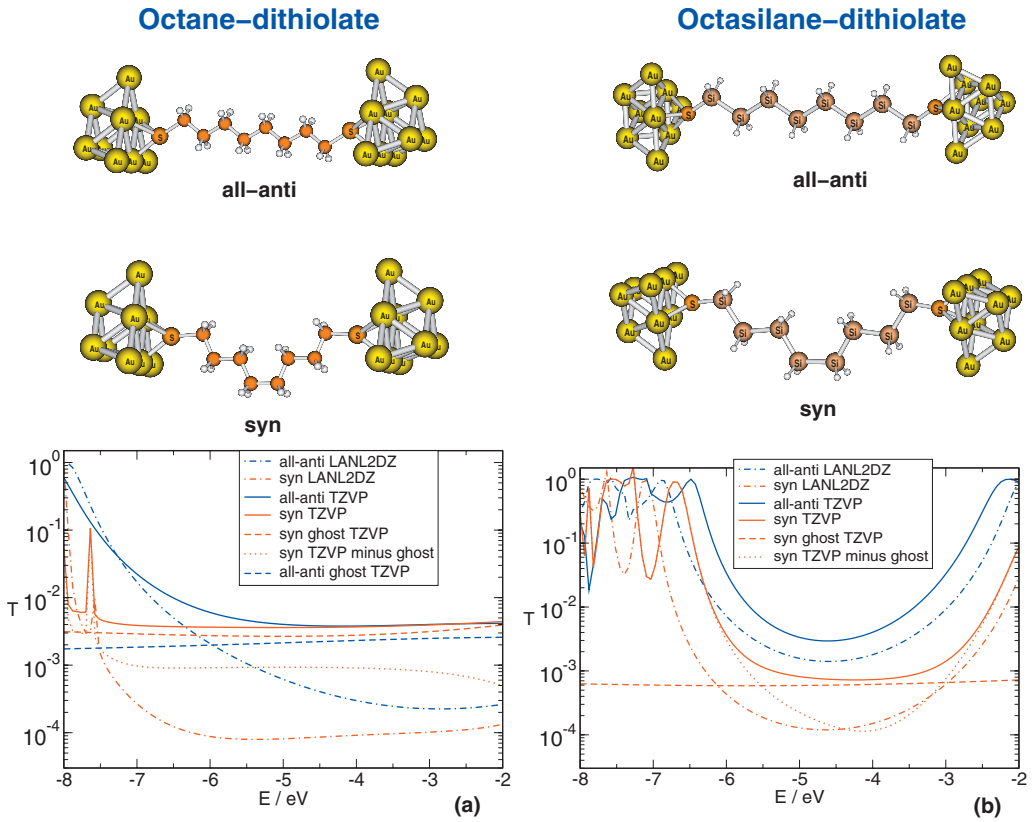

FIG. 3. Transmission for (a) octanedithiolate chains in two different conformations and (b) their silane analogs using Au_9 clusters to mimic the coupling to gold electrodes. The LANL2DZ ghost transmission is in all cases too low to be displayed. KS-DFT(BP86); various Gaussian-type atom-centered basis sets. Electronic structure program: QCHEM.

for the *syn* conformation suggests that the transmission predicted by the full TZVP calculation is not the molecule-specific one we are interested in (see also Sec. VI for further discussion). Thus, it is possible that ghost transmission may *qualitatively* alter predictions in transport calculations. Of course, the importance of the ghost basis problem is system specific. For instance, for the analogous silane (right-hand side of Fig. 3), the TZVP curve for the *syn* conformation shows the typical flat region characteristic of significant ghost transmission, leading to quantitative differences between the TZVP and the LANL2DZ basis sets. Nonetheless, the same qualitative conclusions—that the all-*anti* conformation has a higher transmission over a broad energy range—can be drawn from both basis sets.

When relating the ghost transmission at the estimated Fermi energy of −5.0 eV for the alkane and the silane in the *syn* conformation to the distance between the gold electrodes (14.36 Å for the alkane and 19.84 Å for the silane), a (somewhat naive) decay constant of 0.28 $Å^{-1}$ is obtained, which is close to the value of 0.35 $Å^{-1}$ obtained in a more consistent fashion in the supplementary material.[63] Of course, as will be discussed in Sec. VI, both values are far from typical decay constants for vacuum junctions, and thus the exponential decay alone should not be interpreted as giving ghost transmission physical relevance.

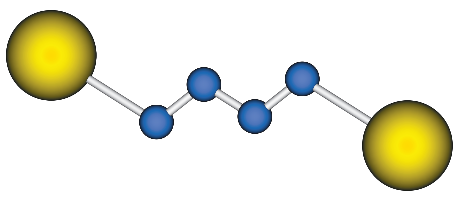

FIG. 4. Ball-and-stick model of the Au—H_4^{ghost}—Au model junction.

For the *syn*-silane, subtracting the ghost transmission from the TZVP curve brings it close to the LANL2DZ curve and thus at least partially fixes the problem (assuming that the errors introduced by the incompleteness of the LANL2DZ basis set are smaller than the ones introduced by ghost transmission for the TZVP basis set). In the case of the alkanes, however, subtracting the ghost transmission obviously still leads to the qualitative conclusion that both conformations have the same transmission. The corrected curve for the *syn* conformation (which is shown on the left-hand side of Fig. 3) also deviates by about an order of magnitude from the LANL2DZ one. Thus, while it appears as a practical approximate way to correct for ghost transmission by subtracting it in cases where ghost transmission is only moderately (up to an order of magnitude) higher than the full transmission (as estimated by the LANL2DZ curve), this method is not applicable to more critical cases such as the alkanes discussed here.

IV. EXPLAINING GHOST TRANSMISSION IN A SMALL MODEL SYSTEM

While it may appear that a practical solution is to calculate the ghost transmission for each junction and subtract it

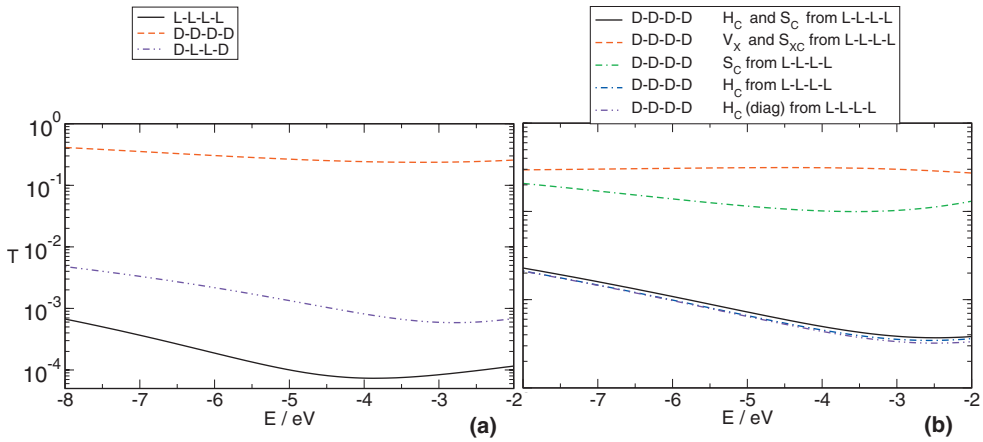

FIG. 5. Transmission for the Au—H_4^{ghost}—Au model junction using (a) different exponents for the four *s*-type Gaussian basis functions and (b) different combinations of matrix blocks. *D* and *L* refer to exponents of 0.1 a.u.$^{-2}$ (diffuse) and 1.0 a.u.$^{-2}$ (local), respectively. See Fig. 1 for definitions of the matrix blocks. KS-DFT—BP86/TZVP(Au), *s*-type ghost basis function (H).

from the full transmission, it is mandatory to understand why ghost transmission is generated to be able to prevent it from leading to erroneous predictions. The possible causes of ghost transmission could include self-interaction errors in the approximate exchange-correlation functional, problems stemming from an improper use of pseudopotentials, qualitative changes in the electron density distribution, near linear dependencies in the basis set, or overlap between basis functions centered on the two electrodes. All of the aforementioned possibilities have been excluded, however, by identifying cases of molecular junctions with a significant ghost transmission when using density functionals with different exact exchange admixture and when using frozen cores instead of pseudopotentials (see Fig. 9), as well as by checking the partial charges on the atoms close to the interface, the condition number of the overlap matrix for the central subsystems, and the largest elements of the electrode-electrode blocks of Fock and overlap matrix (see supplementary material).[63]

In order to elucidate the cause of ghost transmission, we have chosen a model system similar to the one schematically depicted in Fig. 2: it consists of a Au—H_4^{ghost}—Au junction with a zigzag structure (see Fig. 4), where H^{ghost} refers to a ghost atom with only one *s*-type Gaussian basis function with varying exponents centered on it. For the gold atoms, the same TZVP basis set employed in the calculations in Sec. III is used. The interatomic distances have been set to d(H—H)=1.01 Å and d(H—Au)=2.09 Å, and all "bond" angles were chosen to be 109.4° (the linear analog suffered from SCF convergence issues).

As shown in Fig. 5, when using a comparatively large exponent of 1.0 a.u.$^{-2}$ (and thus "local" functions, denoted by L in Fig. 5) for the basis functions on the ghost atoms, the ghost transmission is low in the energy range from −8 to −2 eV. When choosing a smaller exponent of 0.1 a.u.$^{-2}$, and thus more "diffuse" (D) ghost basis functions, the ghost transmission values are considerably higher (around 0.3 instead of around 10^{-4} to 10^{-3}).

The differences observed must stem from either the Fock or the overlap matrix in Eqs. (4) and (5). As can be seen from the right-hand side of Fig. 5, after replacing the coupling blocks of both the overlap and the Fock matrix ($\mathbf{S}_{XC}$ and $\mathbf{V}_X$; see definitions in Fig. 1) in the D-D-D-D calculation by those from the L-L-L-L one, the high transmission remains essentially unchanged, so the coupling parts do not seem to be responsible (at least not alone). When replacing the central part of both matrices, however, the transmission goes down considerably. To determine whether this is due to the Fock or the overlap matrix, both have been replaced individually. While the transmission curve with the central part of the Fock matrix replaced nearly coincides with the one obtained when both matrices were replaced, the one with the central part of the overlap matrix replaced is still very high, so it may be concluded that it is mainly the central part of the Fock matrix which is responsible.

From the Fock matrices of the central region, which are given in Table I, it can be seen that the main difference between the two are the values on the diagonals: while the orbital energies are slightly negative or slightly positive for

TABLE I. Central subsystem Fock matrix for the small-exponent ("D") and the large-exponent ("L") calculations. Entries are given in eV.

	D-D-D-D				L-L-L-L			
	H(1)	H(2)	H(3)	H(4)	H(1)	H(2)	H(3)	H(4)
H(1)	−1.566	−0.730	−0.042	−0.542	36.122	−1.983	−0.735	−0.003
H(2)	−0.730	0.754	0.769	−0.042	−1.983	38.387	−1.582	−0.735
H(3)	−0.042	0.769	0.754	−0.730	−0.735	−1.5832	38.387	−0.983
H(4)	−0.542	−0.042	−0.730	−1.566	−0.003	−0.735	−1.983	36.122

TABLE II. Γ_L and Γ_R at $E=-5.0$ eV for the individual eigenvectors (MOs) of the central subsystem for the small-exponent (diffuse) and the large-exponent (local) calculations. Entries are given in eV.

	D-D-D-D			L-L-L-L			D-L-L-D		
MO	ϵ_i	Γ_R	Γ_L	ϵ_i	Γ_R	Γ_L	ϵ_i	Γ_R	Γ_L
1	−2.94	742.80	742.80	26.76	0.74	0.74	−1.74	323.54	323.56
2	−1.88	585.17	585.16	32.89	1.28	1.28	−1.61	584.5	584.50
3	3.68	11.07	11.07	43.57	0.78	0.78	36.52	46.95	46.95
4	4.16	256.30	256.30	53.94	0.19	0.19	48.90	13.29	13.29

the calculation with the high ghost transmission (D-D-D-D), they are strongly positive for the one with the low ghost transmission (L-L-L-L).

By replacing only the values of the diagonal elements of the central subsystem's Fock matrix in the D-D-D-D calculation by the approximate values of the corresponding elements in the L-L-L-L calculation (37.0 eV), the ghost transmission is brought down significantly to a curve that coincides with the one obtained by replacing the whole central region Fock matrix (see right-hand side of Fig. 5). Also, if the central Fock matrix of the D-D-D-D calculation is substituted into the L-L-L-L one, the transmission goes up by orders of magnitude. This suggests that the diagonal elements of the central region's Fock matrix are mainly responsible for the high ghost transmission. To check again the contribution of the more diffuse basis functions to a potentially larger coupling, the diffuse basis functions were used on the two ghost atoms closest to the gold atoms only, while the two middle ones were described using the local basis function. This results in a fairly low ghost transmission (see left-hand side of Fig. 5), again pointing to a minor role of the coupling. However, given that the combination of the L-L-L-L central Fock and overlap matrices with the electrode-central region coupling blocks from the D-D-D-D calculation does not bring the transmission to the same low values as the original L-L-L-L calculation, it is clear that the coupling, although not solely responsible, does play a role in ghost transmission.

To determine which MOs are responsible for the high transmission in the small-exponent calculation (D-D-D-D), the transmission through the individual central subsystem MOs has been calculated (see Appendix B for details). Since formally there are no electrons on the central subsystem, all MOs are virtuals. It turns out that for the small-exponent calculation (D-D-D-D), MOs 1, 2, and 4 have a transmission of 1 over the whole energy range under study (−8.0 to −2.0 eV), whereas MO 3 has a slightly lower one (0.62 at $E=-5.0$ eV). The transmission close to 1 obtained for the individual MOs can be understood from the coupling of these MOs to the electrodes, i.e., from the matrices $\mathbf{\Gamma}_L$ and $\mathbf{\Gamma}_R$ which in the case of transport through individual MOs are simply numbers Γ_L and Γ_R (see Table II): these are considerably smaller for MO 3 than for the others.

Note that the total transmission is not the sum of transmissions through individual MOs. Thus, when the subsystem MOs with individual transmissions of 1 are considered together, the transmission may be considerably lower than 1. For a Au—H_4^{ghost}—Au model junction with the diffuse function on the ghost atoms adjacent to the gold atoms only (D-L-L-D) there are two strongly coupled and two weakly coupled MOs. The strongly coupled ones have a transmission of nearly 1 each over the energy range under study when considered individually, but the transmission through a system consisting of both MOs is considerably lower than that ($T(-5.0\ \text{eV})=1.4\times10^{-3}$). Combining a high-coupling MO with a low-coupling one leads to a constant transmission of 1, however. The two high-coupling MOs differ from each other in symmetry—one is symmetric and one is antisymmetric with respect to the mirror plane normal to the transport direction, thus resembling a bonding-antibonding MO pair (see rightmost panel in Fig. 6). This is why their contributions to the transmission can cancel although the individual MOs have a transmission of 1 (for a discussion of orbital contributions to transmission and cancellation of these contributions through interference, see, for example, Refs. 20–23 and 86). On a side note, the MOs displayed in Fig. 6 also explain why in the D-D-D-D calculation, the coupling, and thus the transmission of MO 3, is smaller than for the other MOs: this MO is more strongly localized on the central subsystem.

If the coupling terms to the left and to the right electrodes are equal ($\Gamma_L=\Gamma_R=\Gamma$, as in the examples above), so that

$$\Gamma_L=\tfrac{1}{2}(\Gamma_R+\Gamma_L)=\Gamma, \tag{7}$$

the transmission through one central subsystem MO j can be written as

$$\begin{aligned} T(E) &= \Gamma G^r_{jj}(E)\Gamma G^a_{jj}(E) \\ &= \Gamma\cdot\frac{1}{E-\epsilon_j-i\Gamma}\cdot\Gamma\cdot\frac{1}{E-\epsilon_j+i\Gamma} \\ &= \frac{\Gamma^2}{(E-\epsilon_j)^2+\Gamma^2}, \end{aligned} \tag{8}$$

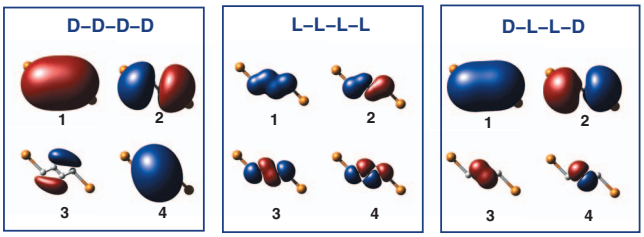

FIG. 6. Isosurface plots of the central subsystem MOs of the Au—H_4^{ghost}—Au model junction (see Appendix B for a definition of subsystem MOs).

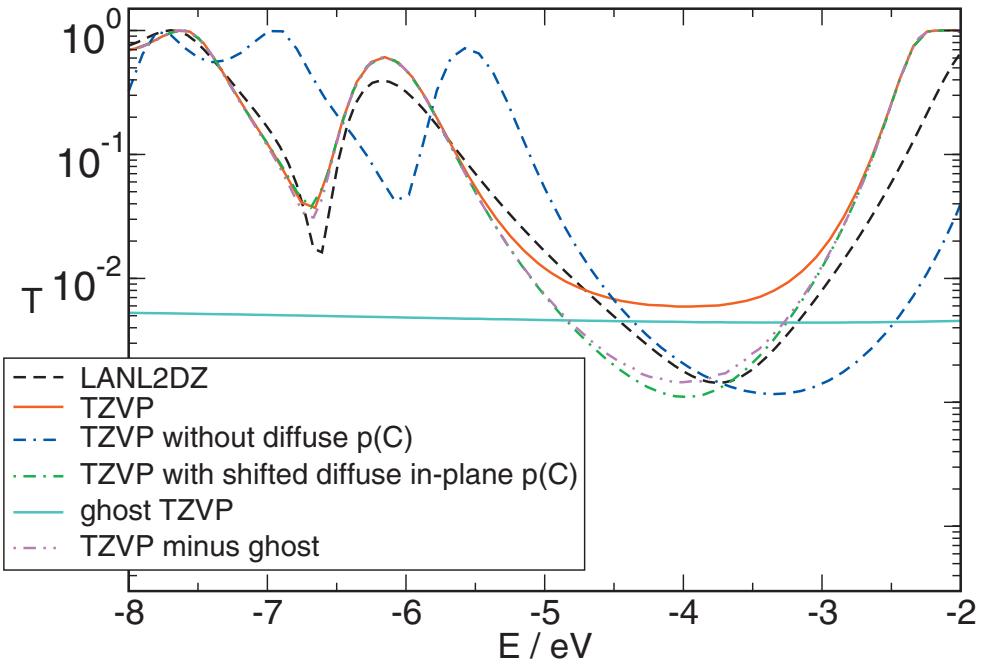

FIG. 7. Transmission for the *meta*-connected benzene derivatives using Au_9 clusters to mimic the coupling to gold electrodes. KS-DFT(BP86); various Gaussian-type atom-centered basis sets. Electronic structure program: QCHEM.

which, for absolute values of Γ considerably larger than the difference between the MO eigenvalue and the energy E, leads to a transmission close to 1 over a certain energy range.

The calculations on the Au—H_4^{ghost}—Au model junction suggest that the major contribution to a high ghost basis transmission arises from small diagonal elements of the central subsystem Hamiltonian (and a subsequent downshift of the energies of the central subsystem MOs). However, it cannot be excluded that a large coupling of the central subsystem to the electrodes is a necessary prerequisite for ghost transmission.

V. IMPLICATIONS FOR MOLECULAR JUNCTIONS

To check whether the conclusions drawn for the small model systems can be applied to realistic molecular junctions, ghost transmission has been investigated for a benzene molecule coupled to the electrodes via ethynyl thiolate spacer groups in the *meta* position. This system has been chosen for three reasons. (1) It is known to have a much lower transmission than its *para*-connected analog,[21,87,88] and is thus more sensitive to parameter effects. (2) In contrast to the alkanes and silanes investigated in Sec. III, where the two systems of interest differ in their conformation, which is hard to control experimentally,[89,90] phenyl rings with different substitution are much more accessible to experimental studies. (3) It has an interesting combination of transport through MOs of σ and π symmetry.[22,91] Since the data discussed in Sec. III involve systems where all bonds are σ bonds, it is an open question whether ghost transmission affects π-conducting molecular bridges to the same extent.

A. Basic considerations

As can be seen in Fig. 7, ghost transmission is significant in the *meta*-connected benzene system when using the TZVP basis set, and leads to full transmission values up to almost an order of magnitude above the ones obtained from the LANL2DZ calculation.

However, when only the most diffuse functions in the TZVP basis set on the carbon atoms, which have p symmetry, are left out in the electronic structure calculations, the transmission goes down to values even below the LANL2DZ ones. Therefore, it may be concluded that these diffuse basis functions are responsible for the ghost transmission, and, if the results from Sec. IV apply for realistic systems, then shifting the diagonal parts of the original TZVP Fock matrix for these basis functions from their original values of about −13 eV to higher values (0 eV in our example) should bring the transmission down. Indeed it does, and it also does so when only shifting the elements for the two "diffuse" p basis functions oriented in the molecular plane, i.e., the ones that contribute to the σ MOs (the latter curve is shown in Fig. 7). Thus, it may be concluded that ghost transmission tends to affect the σ system more than the π system. Note however that for the *meta*-connected benzene, the σ system is the major contributor at low voltages due to interference in the π system.[20,21]

Again, the question arises whether the ghost transmission can be traced back to individual subsystem MOs. In contrast with Sec. IV, we concentrate on the full transmission instead of the ghost one, keeping in mind that the unaltered TZVP calculation is the only one of those summarized in Table III which shows significant ghost transmission. This allows the role of occupied versus virtual subsystem MOs to be assessed. The most striking difference in the MOs of the central subsystem between the unaltered TZVP calculation and the one with the "diffuse" p functions on C removed are the energies: leaving out the "diffuse" basis function leads to upward shifts in virtually all orbital energies (see Table III for representative examples; the LANL2DZ results are also

TABLE III. Energies and couplings Γ_L and Γ_R at the Fermi energies for the individual eigenvectors (MOs) of the central subsystem. Energies are given in eV. The assignments HOMO and LUMO are given by similarities in shape with the corresponding MOs calculated for the isolated molecule.

i	MO	ϵ_i	Γ_R	Γ_L	$T(E_F)$
		TZVP			
50	HOMO−1	−6.29	106.54	106.54	1.00
51	HOMO	−6.05	140.57	140.57	1.00
52	LUMO+2	−2.93	956.92	957.43	1.00
53	LUMO+3	−2.76	963.62	963.33	1.00
54	LUMO	−2.69	268.03	268.07	1.00
55	LUMO+1	−2.31	324.42	324.42	1.00
		LANL2DZ			
40	HOMO−1	−6.08	3.54	3.54	0.70
41	HOMO	−5.77	3.68	3.68	0.77
42	LUMO	−2.09	1.95	1.95	0.58
43	LUMO+1	−1.67	1.59	1.59	0.37
		TZVP without "diffuse" $p(C)$			
50	HOMO−1	−5.47	33.58	33.58	1.00
51	HOMO	−5.18	34.01	34.01	1.00
52	LUMO	−1.52	32.89	32.89	1.00
53	LUMO+1	−1.10	33.15	33.15	1.00
54	LUMO+2	−0.38	531.94	531.97	1.00
55	LUMO+3	−0.21	625.72	625.68	1.00
		TZVP with in-plane $p(C)$ shifted			
50	HOMO−1	−6.29	106.55	106.55	1.00
51	HOMO	−6.05	140.57	140.58	1.00
52	LUMO	−2.69	268.04	268.08	1.00
53	LUMO+1	−2.31	324.43	324.42	1.00
54	LUMO+7	−0.89	432.33	432.37	1.00
55	LUMO+2	−0.56	641.43	641.70	1.00

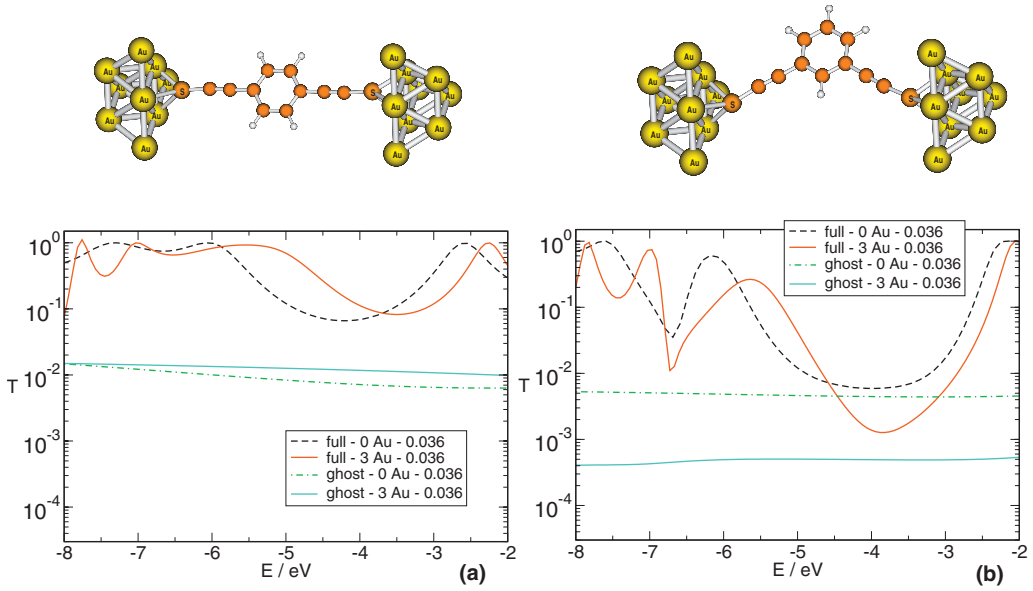

FIG. 8. Influence of the EM size on transmission functions for (a) *para*- and (b) *meta*-connected benzene derivatives using Au_9 clusters to mimic the coupling to gold electrodes. KS-DFT(BP86), TZVP. Electronic structure program: QCHEM.

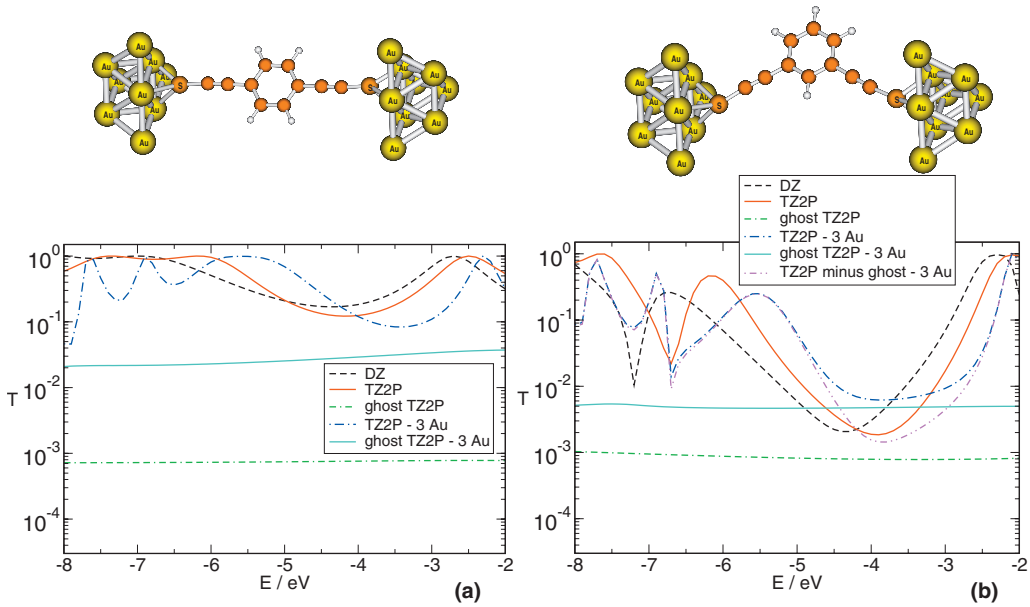

FIG. 9. Influence of the EM size on the transmission functions for (a) *para*- and (b) *meta*-connected benzene derivatives using Au_9 clusters to mimic the coupling to gold electrode. KS-DFT(BP86) in combination with the scalar-relativistic ZORA approximation; small frozen cores; TZ2P basis set (DZ for comparison). Electronic structure program: ADF.

given for comparison). Note that the assignments "HOMO" and "LUMO" are given by similarities in shape with the corresponding MOs calculated for the isolated molecule. Also, the order of the orbitals changes: while in the TZVP calculation without "diffuse" functions, the energetic ordering of the subsystem MOs corresponds to the one in the isolated system, the LUMO+2 and the LUMO+3 replace the LUMO and LUMO+1 when including these functions. The same qualitative picture of orbital shifts is also seen when performing analogous calculations with the two basis sets on isolated benzene, so the shifts are not caused by the molecular junction setup.

Interestingly, the energies as well as the couplings of the HOMO−1 to LUMO+1 in the calculation with the Fock matrix elements of the in-plane "diffuse" *p* functions on C shifted are nearly the same as in the unaltered TZVP calculation. The difference is rather the energies and the order of the "virtual" subsystem MOs above the LUMO+1, which are at higher energies than the ones from the nonshifted calculation. In other words, shifting the "diffuse" *p* functions causes the LUMO+2 and LUMO+3 to move out of the HOMO-LUMO gap.

The implication of these results is that the energetically low-lying virtual subsystem MOs are causing the ghost transmission. The couplings are large enough in both cases to result in transmission of 1 over the energy range considered, so large couplings do not appear to be a sufficient (but presumably a necessary) condition for ghost transmission. Furthermore, the assignments of the HOMO, LUMO, etc. are made based on a TZVP calculation on the isolated molecule in its dithiol form. Thus, the reordering of the virtual subsystem MOs in the TZVP calculation on the junction must be due to the effect of the gold clusters on the central subsystem, and thereby the electrode-molecule couplings also have an indirect influence on the ghost transmission.

In analogy to the D-L-L-D calculation carried out in Sec. IV, we performed calculations using the TZVP basis set on certain parts of the metal-molecule-metal system and the LANL2DZ basis set on others (see supplementary material for details).[63] The conclusions from this study were that it is essential to have the TZVP basis set on *all* atoms in the central region to obtain significant ghost transmission, whereas it only makes a minor difference which basis set is chosen for the gold atoms. Also, having the large basis set on the gold atoms and all molecular atoms close to the interface does not lead to ghost transmission, so that a larger electrode-molecule coupling due to the larger basis set cannot be the sole factor responsible for ghost transmission.

B. Influence of the basis function type and the size of the extended molecule

Another aspect of ghost transmission is its sensitivity to the type of basis set (Slater versus Gaussian functions) and the size of the extended molecule (EM) (molecule only versus three gold atoms included on each side).

In all calculations so far, the central region, i.e., the EM, included the dithiolate molecule only. As shown on the right-hand side of Fig. 8, including the three gold atoms closest to the thiolate adsorption site in the EM causes the ghost transmission to be insignificant when using the Gaussian-type basis set.

However, it increases from an unproblematic to a significant contribution when performing the analogous ADF calculations employing the Slater-type TZ2P basis set (see right-hand side of Fig. 9). This illustrates that it is very difficult to predict whether or not ghost transmission will play a role for a given calculation, and in particular there is no systematic influence of either the size of the EM or the type of basis functions employed.

On the left-hand sides of Figs. 8 and 9, transmission data are also given for the *para*-connected benzene system. The

ghost transmission is always sufficiently well below the full transmission in the *para* system to be considered as insignificant. The comparison to the *meta*-connected system, as well as to the ghost transmission curves for the alkane in two different conformations on the left-hand panel of Fig. 3, suggests that for similar molecules ghost transmission is often, but not always, of the same order of magnitude. It also reinforces the conclusion drawn in Sec. V A that the π system has fewer ghost transmission problems than the σ system.

For all calculations on *meta* benzene where ghost transmission plays a role, subtracting it from the full transmission brings the resulting curve close to the one obtained with the LANL2DZ basis set. This suggests that the simple correction scheme introduced in Sec. III is indeed reasonable for cases where the ghost transmission is not significantly larger than the full transmission obtained from a small basis set.

VI. DISCUSSION: GHOST TRANSMISSION AS A BIASED DESCRIPTION OF VACUUM TUNNELING

Ghost transmission is one cause for the counterintuitive result that transport calculations can lose quality as the atom-centered basis set is enlarged. Of course, the static electronic structure calculations on the metal-molecule-metal system do become more accurate, but this is not necessarily true for the calculation of transport properties based on them.

As discussed in Secs. IV and V, the main reason for this is the appearance of low-energy virtual MOs of the central subsystem when introducing diffuse basis functions. Two types of virtual MOs may be distinguished:[92] (1) chemically relevant virtual MOs (such as antibonding MOs in a diatomic molecule) and (2) virtual MOs arising from the basis functions that go beyond a minimal basis set. These may be called valence virtual and hard virtual MOs, respectively (see Ref. 92 and compare also Refs. 93 and 94 and references therein). In the limit of a complete basis set, the latter would describe the continuum of unbound solutions to the HF or KS equations, and for a system with negative electron affinity, the LUMO should be of that type, having an energy of zero.[95] Altogether, the physical significance of virtual MOs must be considered more questionable than occupied MOs, since they are not variationally optimized.

As pointed out in Ref. 95, there are two types of atom-centered basis functions which can lead to continuumlike virtual MOs: (1) very diffuse basis functions and (2) basis functions centered on "dummy" atoms at some distance from the molecule (i.e., ghost basis functions). The ghost basis calculations are an extreme example of the second case, and all the subsystem MOs are by definition "continuum MOs" (since there are no bonds and therefore no antibonding MOs). Thus, it must clearly be continuum MOs which are responsible for the high transmission in the ghost basis calculations.

As mentioned in Sec. I, there are other areas in computational physics and chemistry where considering larger basis sets does not necessarily lead to better results.[62] In principle this is true of the calculation of any nonvariational property such as, e.g., response properties or transmission functions, for which virtual MOs play a significant role. Apart from sum rules, there is often no general criterion as to how to estimate the error introduced by changing the size of the basis set.

Since there is no molecule in the junction in a ghost transmission calculation, it corresponds to pure through-space (or vacuum) transmission. In principle, the presence of ghost transmission could thus have some physical basis. This is also supported by the fact that when elongating the junction, an exponential decay of ghost transmission is predicted (see Section III and supplementary material).[63] However, the decay constants of 0.28 and 0.35 $Å^{-1}$ obtained for ghost transmission in Sec. III and in the supplementary material,[63] respectively, are much lower than the $3-5$ $Å^{-1}$ typically reported for vacuum tunneling,[96] and also less than half the value of typical decay constants for alkanes.[97]

Furthermore, it is unexpected that pure through-space transmission should dominate the transport properties of molecules such as *meta*-connected benzene systems (although it cannot be strictly excluded, since controlling the interelectrode distance when measuring pure vacuum transport is difficult, so that no reliable experimental reference data are available). The results discussed in Secs. III–V thus suggest that although of relevance in principle, the magnitude of the through-space transmission may be overestimated considerably by the transport approach employed here in combination with an extended atom-centered basis set.

Whether the transmission will converge to a meaningful result in the limit of a complete basis set is a difficult question for several reasons. First, for a basis of atom-centered Gaussian or Slater-type functions, it is not clear how a complete basis that can describe unbound states in an appropriate way should be constructed in practice. For example, is it more important to add diffuse functions centered on the atoms, or should dummy atoms be introduced? How small do the exponents need to be, and which l quantum numbers need to be considered? There is no obvious way of answering these questions analytically, and it may be anticipated that attempts to address them numerically will be hindered by linear dependencies in the basis set. Furthermore, the partitioning problem (see below) may become more important when adding functions with larger exponents, and it is unclear to what extent this may counteract a possible beneficial effect of increasing the basis set. One way to avoid the problems associated with atom-centered basis sets would be to employ a basis of appropriately spaced grid points. This would appear to be a more straightforward way to deal with through-space transmission, and might avoid the ghost transmission problem altogether. Such numerical basis sets have been employed in connection with DFT calculations,[98] and it will be very interesting to see how they perform in combination with transport calculations. A practical drawback here is the fact that these calculations may require a large computational effort, so that in practice often smart grids are used with an increased density of points in regions of high electron density, which again introduces a certain bias.

Another issue which may contribute to an unbalanced description of vacuum transmission is the fact that the interface through which electron transport is calculated is basis set dependent and becomes less and less well defined when

enlarging an atom-centered basis set. When performing transport calculations, the goal is to calculate the rate of charge flow through an interface between an electrode and the central subsystem, defined in three-dimensional Cartesian coordinate space. However, the charge flow actually calculated using Eqs. (1)–(6) is the one between subspaces of the Hilbert space of basis functions. The larger the atom-centered basis set, the more Slater- or Gaussian-type basis functions with small exponents, i.e., with a large spatial extent, will usually be included. In particular, basis functions centered on atoms close to the electrode-central subsystem interface will have significant values on the other side of the interface. This partitioning problem may affect the coupling of central subsystem MOs to the electrodes, which in turn may affect the way the virtual MOs contribute to ghost transmission. Thus, it seems a worthwhile goal for future work to solve this problem in a way which avoids any mixing of central subsystem and electrode basis functions (for one such approach, which, however, does not avoid the mixing entirely, see, e.g., Ref. 68).

For the sake of completeness, it should also be mentioned here that problems may occur because when combining the Landauer approximation with KS-DFT calculations, effective transport of noninteracting fermions (instead of electrons) is described.[44] Furthermore, it is not clear how well MOs obtained from approximate exchange correlation functionals designed to yield accurate total energies are suited for describing transport properties. Recent work by Van Voorhis *et al.* suggests that common exchange-correlation functionals are not suitable for transport calculations because of their local nature.[99] However, when employing the exact functional, the KS MO energies may be interpreted as ionization energies.[100–102]

VII. CONCLUSION AND OUTLOOK

When performing transport calculations within the Landauer approximation, in combination with a NEGF approach using KS-DFT, we have made the counterintuitive observation that transmission obtained by employing a larger basis set is often to be trusted less than that obtained using a smaller basis. The reason for this unexpected result has been identified as ghost transmission. Ghost transmission was defined as the non-negligible transmission (up to 0.3 in the model systems investigated here) obtained from transport calculations in which the central subsystem part consists of ghost basis functions only, i.e., without atomic nuclei or molecular electrons in the central region. The similarity between the nearly energy-independent ghost transmission and flat regions of transmission curves obtained in regular transport calculations with extended basis sets suggested that ghost transmission was also present in the latter. Our results pointed to low-energy virtual MOs of the central subsystem as the cause for ghost transmission. Since these virtual MOs do not give a good description of the continuum of unbound single-electron states, ghost transmission may be interpreted as an inaccurate description of through-space (or vacuum) tunneling. Large couplings between the central region and the electrodes could not be excluded as equally meaningful culprits, but are surely not the only source of ghost transmission.

At the same time, relatively small changes, such as omitting only one set of p basis functions, using a smaller basis set on a few atoms only, employing Slater-type instead of Gaussian-type basis functions, or enlarging the central region from including zero to including three gold atoms on each side, have been shown to yield considerable changes in the importance of the ghost transmission. Thus, for a given calculation, we cannot in general predict whether ghost transmission will change qualitative conclusions or not. However, the following may be regarded as rough rules of thumb: so far, we have never obtained a significant ghost transmission for a calculation employing a basis set of double-zeta quality without polarization functions. On the other hand, ghost transmission is particularly likely to occur when using basis functions with comparatively small exponents (such as 0.1 a.u.$^{-2}$ in p-type Gaussian functions). Furthermore, ghost transmission affects transport through orbitals of σ symmetry considerably more than those of π symmetry. Finally, the larger the distance between the electrodes, the smaller the values of ghost transmission tend to be (which, of course, also holds for through-MO transmission).

In general, flat parts in the transmission as a function of energy may suggest significant ghost transmission (although such features have also been found when the dominant contribution to transmission changes from the π to the σ system in cases of π interference[20]). *As a simple heuristic remedy, it may then be recommended to subtract the ghost transmission from the full transmission*. Fortunately, although the convergence of the SCF algorithm may be difficult in some cases, loose convergence criteria do not seem to alter ghost transmission curves to a large extent. While this correction may prove to be of little value in cases where the ghost transmission is more than one order of magnitude larger than the full transmission calculated from a small basis set, it may provide a good approximation for the true transmission in other affected cases.

Another conclusion from this work is that molecules with interference features in the transmission, such as *meta*-connected benzene derivatives, as well as other low-conducting systems such as alkanes, are considerably more sensitive to basis set effects (and presumably to other parameters of the calculation) than those which have a consistently high transmission over the energy range of interest. Therefore, basis set studies should be carried out on these sensitive molecules rather than on their more robust counterparts.

The numerical agreement between calculated ghost transmission and full transmission in all "problematic" cases discussed in Secs. III and V suggests that ghost basis calculations can lead to a good estimate of the way in which a larger basis set modifies the contribution of the virtual MOs. MO interference[20,22] makes it hard, however, to settle this issue satisfactorily by considering transmission through subsets of MOs, and thus deciding to what degree modifications of the chemically relevant virtual MOs are responsible for the ghost transmission, and to what degree the increasing number of hard virtuals leads to problems.

Altogether it becomes clear that when used blindly, the implementation of the Landauer approach adopted here may not be suitable for large nonorthogonal atom-centered basis sets as commonly used in quantum chemistry. This adds to the other computational and formal uncertainties which may prevent this implementation from giving quantitatively reliable results. These include the band alignment problem, conceptual issues with KS-DFT, and self-interaction errors in exchange correlation functionals (also called delocalization errors[103]). To circumvent difficulties when using large atom-centered basis sets, a better description of the vacuum may be needed to achieve a more balanced description of through-space versus through-bond transmission, for example, by placing an array of ghost basis functions between the electrodes, or by employing a numerical grid or plane waves as a basis. It may also be necessary to employ a different partitioning strategy to describe the surface through which the transmission (and thus the current) are to be calculated in a more realistic way.

A formal analogy may be made[28–30] between ET in donor-bridge-acceptor systems[104,105] and molecular conduction, and consequently the interpretation of ghost transmission in terms of a biased description of vacuum tunneling may be related to through-space coupling in ET reactions. The effects of basis set size,[106,107] virtual orbital contributions,[108] and bridge length[109] in pathway formulations of bridge-mediated donor-acceptor coupling calculations have been studied, but the connection between large basis sets and an overestimation of through-space coupling has not been discussed in this context. Therefore, the considerations discussed here apply, in principle, to ET reactions and more generally to all cases where electronic coupling via molecular bridges is of importance.

ACKNOWLEDGMENTS

The authors would like to thank Thorsten Hansen, Jeffrey R. Reimers, and Matthew G. Reuter for helpful comments and discussions. C.H. gratefully acknowledges funding by a Forschungsstipendium by the Deutsche Forschungsgemeinschaft (DFG). M.A.R. thanks the Chemistry and Materials Research Divisions (MRSEC program) of the NSF and the DOE for support.

APPENDIX A: A FORMAL PROBLEM WITH THE SIMPLE IMPLEMENTATION OF THE WIDE-BAND-LIMIT APPROXIMATION

In the WBL approximation, the assumption is made that the density of states (DOS) of the electrodes is energy independent, which is a good approximation for gold with its flat DOS around the Fermi energy. In combination with electronic structure calculations, a LDOS is assigned to each basis function centered on a gold atom. Formally, these LDOS values add up to the total DOS (see below), but in actual transport calculations it often turns out that the LDOS for the gold 6*s* band may be assigned to each basis function regardless of its *l* quantum number without significantly altering the results.[83,110] The values chosen for the LDOS in transport calculations employing the WBL approximation are commonly those obtained from DFT calculations under periodic boundary conditions using the local-density approximation.[84] These values sum up to the total DOS when assigned to the functions in a minimal basis set. It is clear, however, that the larger the basis set, the more this sum will exceed the total DOS. Since a larger DOS leads to a larger transmission, this effect may contribute to an overestimation of the transmission function when using large basis sets in combination with the implementation of the WBL approximation presented here.

1. Formal considerations

Equation (6), which defines how the electrode's Green's functions are calculated within the WBL approximation, can be derived as follows. The retarded Green's function operator $\hat{g}(E)$ of a one-electron system described by the Hamiltonian $\hat{h}$ is defined as

$$\hat{g}(E) = \lim_{\eta \to 0+} (E - \hat{h} + i\eta)^{-1}, \tag{A1}$$

which can be expressed in a basis of eigenfunctions $|j\rangle$ of $\hat{h}$ as

$$\hat{g}(E) = \lim_{\eta \to 0+} \sum_j |j\rangle (E - \epsilon_j + i\eta)^{-1} \langle j|, \tag{A2}$$

where ϵ_j is the energy of eigenfunction $|j\rangle$.

The operator $\hat{D}(E)$ associated with the DOS $D(E)$ of the system is defined in the same basis as

$$\hat{D}(E) = \sum_j |j\rangle \delta(E - \epsilon_j) \langle j|. \tag{A3}$$

Of course, the total DOS is obtained as its expectation value, which for a single-Slater determinant wave function reads

$$D(E) = \langle \hat{D}(E) \rangle = \sum_{j,k} \langle k|j\rangle \delta(E - \epsilon_j) \langle j|k\rangle$$
$$= \sum_{j,k} \delta_{jk} \delta(E - \epsilon_j) \delta_{jk} = \sum_j \delta(E - \epsilon_j). \tag{A4}$$

From the definition of the Dirac delta function as

$$\delta(x) = \lim_{\eta \to 0+} \frac{1}{\pi} \frac{\eta}{x^2 + \eta^2}, \tag{A5}$$

the relationship

$$\delta(x) = -\frac{1}{\pi} \lim_{\eta \to 0+} \mathrm{Im}[(x + i\eta)^{-1}] \tag{A6}$$

can be derived, from which it follows that

$$\hat{D}(E) = -\frac{1}{\pi} \mathrm{Im}[\hat{g}(E)]. \tag{A7}$$

The LDOS $D_\mu(E)$, i.e., the DOS projected onto the basis function $|\mu\rangle$ (which may be chosen to be local) can be defined as

$$D_\mu(E) = -\frac{1}{\pi} \mathrm{Im}[g_{\mu\mu}(E)], \tag{A8}$$

which may be reformulated as

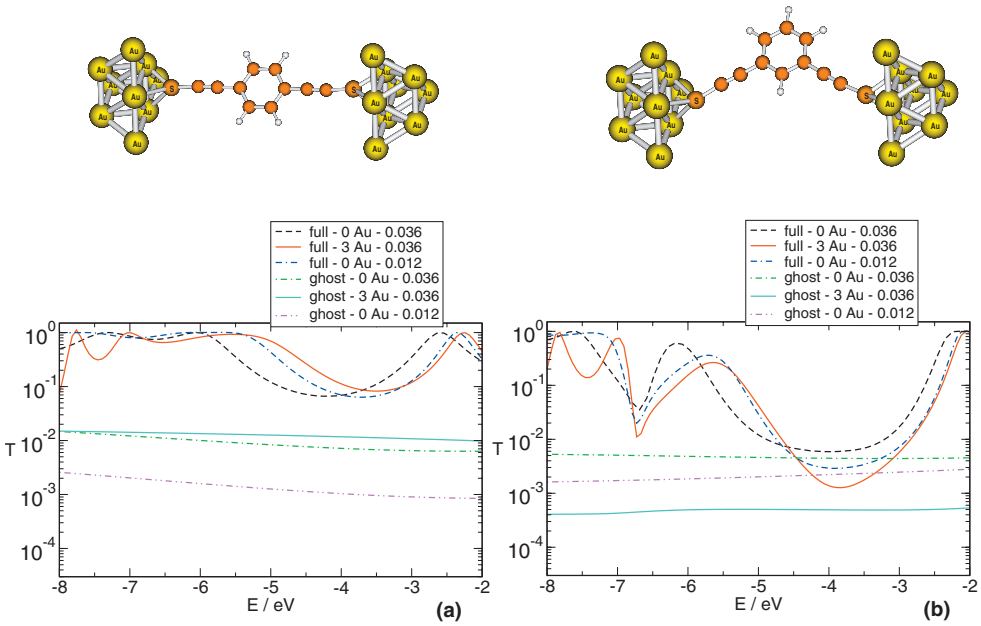

FIG. 10. Influence of the EM size and the LDOS value on transmission functions for (a) *para*- and (b) *meta*-connected benzene derivatives using Au_9 clusters to mimic the coupling to gold electrodes. The values in the legend refer to the constant LDOS in Eq. (6). KS-DFT(BP86), TZVP. Electronic structure program: QCHEM.

$$\mathrm{Im}[g_{\mu\mu}(E)] = -\pi D_{\mu}(E). \tag{A9}$$

By choosing a constant value for $D_{\mu}(E)$ and setting all off-diagonal imaginary and all real terms to zero, Eq. (6) is obtained.

By adding up the LDOS values for all basis functions, the total DOS is recovered,

$$\sum_{\mu} D_{\mu}(E) = D(E). \tag{A10}$$

2. Effect of the LDOS on the transmission

The constant LDOS value of 0.036 eV^{-1} employed throughout this paper is taken from Ref. 84 and corresponds to the DOS of either spin up or spin down electrons, projected onto the 6*s* band of gold. It should be noted that the LDOS value of 0.072 eV^{-1}, which can sometimes be found in the literature, refers to the LDOS for all electrons, not to the spin-resolved one, so it seems reasonable to multiply it by 1/2 when using an effective one-electron picture (compare also Ref. 111).

Since there is no clear prescription on how to distribute the 6*s* LDOS between the two or three basis functions chosen for the 6*s* orbital of gold in a LANL2DZ or TZVP basis set, respectively, we will continue to use the value 0.036 eV^{-1} for all of them. This can be seen in analogy to the way the 6*s* LDOS may be employed for all basis functions regardless of their *l* quantum number without a considerable loss of accuracy.[83,110,111] However, since this does affect the transmission, in particular for systems such as *meta*-connected benzene (see Fig. 10), the possibility of this parameter needing to be adjusted should be kept in mind. Figure 10 is equivalent to Fig. 8, but includes full and ghost transmissions for a LDOS value of 0.012 eV^{-1}, i.e., the 6*s* LDOS is distributed evenly among the three basis functions describing that shell. As to be expected, for the *meta*-connected benzene both the total and the ghost transmission go down compared with the LDOS=0.036 eV^{-1} calculations, although only slightly, and the ghost transmission is still significant. For the *para* system, the full transmission is only shifted, but not diminished.

3. Discussion

One obvious solution to the LDOS problem would be to choose a minimal basis set on the gold atoms—however, it has been reported that using a single-zeta basis set for the electrodes and a double-zeta one with polarization functions for the central subsystem instead of having the larger basis set on all atoms may lead to large changes in the calculated transport properties.[59]

Improving the implementation of the WBL approximation described here would involve recalculating the correct LDOS for each basis function every time a new basis set is employed. This would eradicate the main advantage of the WBL approximation, its computational simplicity while retaining a surprisingly good agreement with conductivities obtained using a tight-binding description of the electrode's Green's functions.[22,112] Also, even with the smallest reasonable LDOS (0.012 eV^{-1}), there is considerable ghost transmission in *meta* benzene (see Fig. 10), so correcting this value alone would not solve the problem.

Altogether, the considerations outlined above make it clear that the uncertainty regarding the correct value for the LDOS does not allow for definitive quantitative predictions to be made from the WBL approach as implemented here. Of course, it may be anticipated that for a reasonable choice of LDOS values, even when sacrificing some quantitative accuracy, qualitative conclusions should be affected only negligibly.

APPENDIX B: TRANSMISSION THROUGH INDIVIDUAL CENTRAL SUBSYSTEM MOs

Subsystem MOs are the solutions to the subsystem's secular equation,

$$\mathbf{H}_C\mathbf{C}_C = \mathbf{S}_C\mathbf{C}_C\boldsymbol{\epsilon}_C, \tag{B1}$$

where $\mathbf{H}_C$ and $\mathbf{S}_C$ are the central subsystem blocks of the total system's Fock and overlap matrices, respectively, the entries in $\mathbf{C}_C$ are the subsystem MO coefficients, $\boldsymbol{\epsilon}_C$ is a diagonal matrix containing the MO energies, and C indicates the central subsystem. To make this manuscript self-contained, the procedure employed for calculating the transmission through an individual subsystem MO shall be briefly summarized: the total system is transformed with a Löwdin orthogonalization on the subsystem,

$$\mathbf{H}'_C = \mathbf{S}_C^{-1/2}\mathbf{H}_C\mathbf{S}_C^{-1/2}, \tag{B2}$$

while adjusting the elements having indices on both an electrode and on the central subsystem accordingly, i.e., the total Hamiltonian and overlap matrix are transformed with a matrix which has the electrode blocks equal to the unit matrix and the central block equal to $\mathbf{S}_C^{-1/2}$, and the off diagonal blocks are all zero. Then, $\mathbf{H}'_C$ is diagonalized by transforming the full system with a transformation matrix of the style described above, but with the $\mathbf{H}'_C$ eigenvectors in the central block. Then, all elements with indices not corresponding to the selected central-subsystem MO are removed from the central subblocks and the central system-electrode coupling blocks of the transformed total Fock and overlap matrices, and a transport calculation is carried out for the remaining system. Of course, this procedure can also be used to evaluate the transmission due to any set of subsystem MOs.

APPENDIX C: COMPUTATIONAL METHODS

Electronic structures of the electrode-molecule-electrode systems were calculated using a finite cluster approach, i.e., without employing periodic boundary conditions. Molecular structures were first optimized for the isolated, twofold negatively charged dithiolate molecules using a 6-311G** basis set[113] and the B3LYP[114,115] density functional. To construct the junctions, the molecules were placed between Au_9 clusters, mimicking the fcc sites of Au(111) surfaces. The sulfur-gold distances were chosen to be 2.48 Å, as predicted from KS-DFT calculations for this binding arrangement,[116] while the gold-gold distances were set to their value in extended gold crystals (2.88 Å). Benzene-based molecules included —C≡C— spacer groups on both sides to minimize direct interactions between the hydrogen atoms of the benzene rings and the gold electrode.

Zero-voltage transmission functions were calculated according to Eq. (1) using a tool written in our laboratory[117] for postprocessing electronic structure calculations. Overlap and Fock matrices were obtained from KS-DFT[44,45] or HF calculations on molecules using a locally modified version of QCHEM[118] or ADF.[119] The effects of the open-boundary conditions and the voltage drop in the molecular junctions were neglected. The self-energy matrices $\boldsymbol{\Sigma}_R$ and $\boldsymbol{\Sigma}_L$ of the gold electrodes were calculated within the WBL approximation (see Sec. II), assuming a constant LDOS of 0.036 eV^{-1} if not indicated otherwise, which corresponds to the LDOS for electrons of a given spin quantum number of bulk gold at the Fermi energy.[84] For the transport calculations, the pure density functional BP86,[120,121] as well as the hybrid functional B3LYP and the HF approximation, was employed. The Los Alamos LANL2DZ effective core potentials[122] and the matching basis sets of double-zeta quality were used as implemented in QCHEM, as well as Ahlrichs' SVP, TZVP, and TZVPP basis sets[123,124] in combination with Stuttgart effective core potentials for gold atoms (which also account for the scalar relativistic effects).[125] SV denotes a split valence and TZV a triple-zeta split valence basis set, and one and two Ps correspond to one or two sets of polarization functions on all atoms, respectively. While all basis sets used in QCHEM calculations were of Gaussian type, the Slater-type basis sets of double and triple-zeta quality with none and two sets of polarization functions, respectively, were used in the ADF calculations (DZ and TZ2P as implemented in ADF). All ADF calculations were carried out within the zeroth-order regular approximation (ZORA) to describe scalar relativistic effects, and were using a small frozen core, comprising the 1*s* shell of carbon atoms and the 1*s* through 4*d* shells of gold atoms. A tight criterion of 10^{-8} a.u. for the direct inversion in the iterative subspace error was chosen in all QCHEM calculations, whereas a criterion of 10^{-6} a.u. was chosen for the largest element of the commutator of the Fock matrix and the density matrix in the ADF calculations.

Since the choice of the value for the Fermi energy of the gold electrodes within the Landauer approximation is not at all obvious within the approach chosen here, and since it does not affect the discussion of parameter dependence of the transmission, energy values were not shifted by the Fermi energy. For a general orientation, while the Fermi function for bulk gold is −5.5 eV,[126] the fact that in practical calculations metal clusters of finite size are used to model the bulk electrodes may shift this value. We restricted the energy range for which transmission is calculated to the interval of −8 to −2 eV, which includes all energy values commonly accessible experimentally. It may also be assumed that this interval encompasses the region around the Fermi energy for which the WBL approximation provides a good description. Löwdin population analyses were carried out by postprocessing QCHEM output with ARTAIOS.[117]

[1] N. S. Hush, Ann. N.Y. Acad. Sci. **1006**, 1 (2003).
[2] A. Aviram and M. Ratner, Chem. Phys. Lett. **29**, 277 (1974).
[3] D. Vuillaume, C. R. Phys. **9**, 78 (2008).
[4] C. A. Mirkin and M. A. Ratner, Annu. Rev. Phys. Chem. **43**, 719 (1992).
[5] A. Nitzan and M. A. Ratner, Science **300**, 1384 (2003).
[6] M. A. Ratner, Mater. Today **5**, 20 (2002).
[7] N. J. Tao, Nat. Nanotechnol. **1**, 173 (2006).
[8] J. R. Heath and M. A. Ratner, Phys. Today **56**, 43 (2003).
[9] C. Joachim and M. A. Ratner, Proc. Natl. Acad. Sci. U.S.A. **102**, 8801 (2005).
[10] A. Nitzan, Annu. Rev. Phys. Chem. **52**, 681 (2001).
[11] B. Ulgut and H. D. Abruña, Chem. Rev. (Washington, D.C.) **108**, 2721 (2008).
[12] *Introducing Molecular Electronics*, Lecture Notes in Physics Vol. 680, edited by G. Cuniberti, G. Fagas, and K. Richter (Springer, New York, 2005).
[13] J. M. Tour, *Molecular Electronics: Commercial Insights, Chemistry, Devices, Architecture and Programming*, Lecture Notes in Physics (World

Scientific, Singapore, 2003).
[14] M. Di Ventra, *Electrical Transport in Nanoscale Systems* (Cambridge University Press, Cambridge, England, 2008).
[15] *Nano and Molecular Electronics Handbook*, Nano- and Microscience, Engineering, Technology and Medicine Vol. 9, edited by S. E. Lyshevski (CRC, London, 2007).
[16] J. Jortner and M. Ratner, *Molecular Electronics* (Blackwell Science, Oxford, 1997).
[17] *Introduction to Molecular Electronics*, edited by M. C. Petty, M. R. Bryce, and D. Bloor (Oxford University Press, New York, 1995).
[18] *Atomic and Molecular Wires*, edited by C. Joachim and S. Roth (Kluwer, Dordrecht, 1997).
[19] *Molecular Electronics II*, Annals of the New York Academy of Science Vol. 960, edited by A. Aviram, M. Ratner, and V. Mujica (The New York Academy of Science, New York, 2002).
[20] G. C. Solomon, D. Q. Andrews, R. P. Van Duyne, and M. A. Ratner, J. Am. Chem. Soc. **130**, 7788 (2008).
[21] G. C. Solomon, D. Q. Andrews, T. Hansen, R. H. Goldsmith, M. R. Wasielewski, R. P. Van Duyne, and M. A. Ratner, J. Chem. Phys. **129**, 054701 (2008).
[22] S.-H. Ke, W. Yang, and H. U. Baranger, Nano Lett. **8**, 3257 (2008).
[23] K. Yoshizawa, T. Tada, and A. Staykov, J. Am. Chem. Soc. **130**, 9406 (2008).
[24] T. Helgaker, P. Jørgensen, and J. Olsen, *Molecular Electronic-Structure Theory* (Wiley, New York, 2000).
[25] C. A. Ullrich and I. V. Tokatly, Phys. Rev. B **73**, 235102 (2006).
[26] E. B. Davies, *Quantum Theory of Open Systems* (Academic, New York, 1976).
[27] S. Datta, *Quantum Transport: Atom to Transistor* (Cambridge University Press, Cambridge, England, 2005).
[28] A. Nitzan, J. Phys. Chem. A **105**, 2677 (2001).
[29] S. Yeganeh, M. A. Ratner, and V. Mujica, J. Chem. Phys. **126**, 161103 (2007).
[30] S. Skourtis and A. Nitzan, J. Chem. Phys. **119**, 6271 (2003).
[31] R. A. Marcus, J. Chem. Phys. **24**, 966 (1956).
[32] R. A. Marcus and N. Sutin, Biochim. Biophys. Acta **811**, 265 (1985).
[33] N. S. Hush, Trans. Faraday Soc. **57**, 557 (1961).
[34] N. S. Hush, Electrochim. Acta **13**, 1005 (1968).
[35] V. Barone, R. Improta, and N. Rega, Acc. Chem. Res. **41**, 605 (2008).
[36] C. Herrmann and M. Reiher, Top. Curr. Chem. **268**, 85 (2007).
[37] D. Frenkel and B. Smit, *Understanding Molecular Simulation*, Computational Science Series Vol. 1 (Academic, New York, 2002).
[38] M. P. Allen and D. J. Tildesley, *Computer Simulation of Liquids* (Oxford University Press, New York, 1989).
[39] S. M. Lindsay and M. A. Ratner, Adv. Mater. (Weinheim, Ger.) **19**, 23 (2007).
[40] R. Landauer, IBM J. Res. Dev. **1**, 223 (1957).
[41] R. Landauer, Philos. Mag. **21**, 863 (1970).
[42] M. Büttiker, Y. Imry, R. Landauer, and S. Pinhas, Phys. Rev. B **31**, 6207 (1985).
[43] G. D. Mahan, *Many-Particle Physics* (Plenum, New York, 1990).
[44] W. Kohn and L. J. Sham, Phys. Rev. **140**, A1133 (1965).
[45] P. Hohenberg and W. Kohn, Phys. Rev. **136**, B864 (1964).
[46] T. Frauenheim, G. Seifert, M. Elstner, T. Niehaus, C. Köhler, M. Amkreutz, M. Sternberg, Z. Hajnal, A. D. Carlo, and S. Suhai, J. Phys.: Condens. Matter **14**, 3015 (2002).
[47] T. Shimazaki and K. Yamashita, Int. J. Quantum Chem. **109**, 1834 (2009).
[48] A. R. Rocha, V. M. García-Suárez, S. Bailey, C. Lambert, J. Ferrer, and S. Sanvito, Phys. Rev. B **73**, 085414 (2006).
[49] Y. Xue, S. Datta, and M. A. Ratner, Chem. Phys. **281**, 151 (2002).
[50] F. Pauly, J. K. Viljas, J. C. Cuevas, and G. Schön, Phys. Rev. B **77**, 155312 (2008).
[51] M. Koentopp, C. Chang, K. Burke, and R. Car, J. Phys.: Condens. Matter **20**, 083203 (2008).
[52] S.-H. Ke, H. U. Baranger, and W. Yang, J. Phys. Chem. **126**, 201102 (2007).
[53] C. W. Bauschlicher, Jr., J. W. Lawson, A. Ricca, Y. Xue, and M. A. Ratner, Chem. Phys. Lett. **388**, 427 (2004).
[54] Y. García, E. San-Sabián, E. Louis, and J. A. Vergés, Int. J. Quantum Chem. **108**, 1637 (2008).
[55] M. Zhuang, P. Rocheleau, and M. Ernzerhof, J. Chem. Phys. **122**, 154705 (2005).
[56] S.-H. Ke, H. U. Baranger, and W. Yang, J. Chem. Phys. **127**, 144107 (2007).
[57] S.-H. Ke, H. U. Baranger, and W. Yang, J. Chem. Phys. **123**, 114701 (2005).
[58] G. C. Solomon, J. R. Reimers, and N. S. Hush, J. Chem. Phys. **122**, 224502 (2005).
[59] S.-H. Ke, H. U. Baranger, and W. Yang, J. Chem. Phys. **122**, 074704 (2005).
[60] M. Strange, I. S. Kristensen, K. S. Thygesen, and K. W. Jacobsen, J. Chem. Phys. **128**, 114714 (2008).
[61] A. D. Boese, J. M. L. Martini, and N. C. Handy, J. Chem. Phys. **119**, 3005 (2003).
[62] J. Nobel, S. Trickey, J. R. Sabin, and J. Oddershede, Chem. Phys. **309**, 89 (2005); M. N. Paddon-Row and K. D. Jordan, *Through-Bond and Through-Space Interactions in Unsaturated Hydrocarbons: Their Implications for Chemical Reactivity and Long-Range Electron Transfer*, in Modern models of bonding and delocalization, edited by J. F. Liebman and A. Greenberg (Wiley VCH, New York, 1989).
[63] See supplementary material at http://dx.doi.org/10.1063/1.3283062 for further data.
[64] C. Caroli, R. Combescot, P. Nozieres, and D. Saint-James, J. Phys. C **4**, 916 (1971).
[65] T. N. Todorov, G. A. D. Briggs, and A. P. Sutton, J. Phys.: Condens. Matter **5**, 2389 (1993).
[66] Y. Meir and N. S. Wingreen, Phys. Rev. Lett. **68**, 2512 (1992).
[67] A. R. Williams, P. J. Feibelman, and N. D. Lang, Phys. Rev. B **26**, 5433 (1982).
[68] K. S. Thygesen, Phys. Rev. B **73**, 035309 (2006).
[69] S.-H. Ke, H. U. Baranger, and W. Yang, Phys. Rev. B **70**, 085410 (2004).
[70] A. Di Carlo, M. Gheorghe, P. Lugli, M. Sternberg, G. Seifert, and T. Frauenheim, Physica B **314**, 86 (2002).
[71] Y. Chen, A. Prociuk, T. Perrine, and B. D. Dunietz, Phys. Rev. B **74**, 245320 (2006).
[72] E. Louis, J. A. Vergés, J. J. Palacios, A. J. Pérez-Jiménez, and E. San Fabián, Phys. Rev. B **67**, 155321 (2003).
[73] M. Ernzerhof and M. Zhuang, Int. J. Quantum Chem. **101**, 557 (2005).
[74] F. Evers, F. Weigend, and M. Koentopp, Phys. Rev. B **69**, 235411 (2004).
[75] A. Arnold, F. Weigend, and F. Evers, J. Chem. Phys. **126**, 174101 (2007).
[76] A. Pecchia and A. D. Carlo, Rep. Prog. Phys. **67**, 1497 (2004).
[77] J. Tomfohr and O. F. Sankey, J. Chem. Phys. **120**, 1542 (2004).
[78] M. Brandbyge, N. Kobayashi, and M. Tsukada, Phys. Rev. B **60**, 17064 (1999).
[79] A. Teklos and S. S. Skourtis, J. Chem. Phys. **125**, 244103 (2006).
[80] Y. Xue, S. Datta, and M. A. Ratner, J. Chem. Phys. **115**, 4292 (2001).
[81] J. Taylor, H. Guo, and J. Wang, Phys. Rev. B **63**, 245407 (2001).
[82] H. Guo, personal communication (2009).
[83] A. Prociuk, B. Van Kuiken, and B. D. Dunietz, J. Chem. Phys. **125**, 204717 (2006).
[84] D. A. Papaconstantopoulos, *Handbook of the Band Structure of Elemental Solids* (Plenum, New York, 1986).
[85] S. F. Boys and F. Bernardi, Mol. Phys. **19**, 553 (1970).
[86] T. Hansen, G. C. Solomon, D. Q. Andrews, and M. A. Ratner, J. Chem. Phys. **131**, 194704 (2009).
[87] M. Mayor, H. B. Weber, J. Reichert, M. Elbing, C. von Hänisch, D. Beckmann, and M. Fischer, Angew. Chem., Int. Ed. **42**, 5834 (2003).
[88] J. J. Sumner and S. E. Creager, J. Am. Chem. Soc. **122**, 11914 (2000).
[89] Y. Hu, Y. Zhu, H. Gao, and H. Guo, Phys. Rev. Lett. **95**, 156803 (2005).
[90] H. Cao, J. Jiang, J. Ma, and Y. Luo, J. Am. Chem. Soc. **130**, 6674 (2008).
[91] G. C. Solomon, D. Q. Andrews, R. P. V. Duyne, and M. A. Ratner, ChemPhysChem **10**, 257 (2009).
[92] J. E. Subotnik, A. D. Dutoi, and M. Head-Gordon, J. Chem. Phys. **123**, 114108 (2005).
[93] I. Mayer, Chem. Phys. Lett. **242**, 499 (1995).
[94] M. S. Lee and M. Head-Gordon, Int. J. Quantum Chem. **76**, 169 (2000).
[95] D. B. Cook, Int. J. Quantum Chem. **60**, 793 (1996).
[96] H. B. Gray and J. R. Winkler, Q. Rev. Biophys. **36**, 341 (2003).
[97] L. Venkataraman, J. E. Klare, I. W. Tam, C. Nuckolls, M. S. Hybertsen, and M. L. Steigerwald, Nano Lett. **6**, 458 (2006).
[98] J. R. Chelikowsky, L. Kronik, I. Vasiliev, M. Jain, and Y. Saad, *Using Real Space Pseudopotentials for the Electronic Structure Problem*, Handbook of Numerical Analysis Vol. 10 (Elsevier, New York, 2003), pp. 613–637.
[99] J. S. Evans, O. A. Vydrov, and T. Van Voorhis, J. Chem. Phys. **131**, 034106 (2009).
[100] D. P. Chong, O. V. Gritsenko, and E. J. Baerends, J. Chem. Phys. **116**,

1760 (2002).
[101] J. P. Perdew and M. Levy, Phys. Rev. Lett. **51**, 1884 (1983).
[102] J. F. Janak, Phys. Rev. B **18**, 7165 (1978).
[103] A. J. Cohen, P. Mori-Sánchez, and W. Yang, Science **321**, 792 (2008).
[104] H. B. Gray and J. R. Winkler, Proc. Natl. Acad. Sci. U.S.A. **102**, 3534 (2005).
[105] M. R. Wasielewski, J. Org. Chem. **71**, 5051 (2006).
[106] W. Kurlancheek and R. J. Cave, J. Phys. Chem. A **110**, 14018 (2006).
[107] C. Liang and M. D. Newton, J. Phys. Chem. **96**, 2855 (1992).
[108] L. A. Curtiss, C. A. Naleway, and J. R. Miller, Chem. Phys. **176**, 387 (1993).
[109] K. D. Jordan and M. N. Paddon-Row, Chem. Rev. (Washington, D.C.) **92**, 395 (1992).
[110] W. Tian, S. Datta, S. Hong, R. Reifenberger, J. I. Henderson, and C. P. Kubiak, J. Chem. Phys. **109**, 2874 (1998).
[111] L. E. Hall, J. R. Reimers, N. S. Hush, and K. Silverbrook, J. Chem. Phys. **112**, 1510 (2000).
[112] C.-L. Cheng, J. S. Evans, and T. Van Voorhis, Phys. Rev. B **74**, 155112 (2006).
[113] R. Krishnan, J. S. Binkley, R. Seeger, and J. A. Pople, J. Chem. Phys. **72**, 650 (1980).
[114] A. D. Becke, J. Chem. Phys. **98**, 5648 (1993).
[115] C. Lee, W. Yang, and R. G. Parr, Phys. Rev. B **37**, 785 (1988).
[116] A. Bilić, J. R. Reimers, and N. S. Hush, J. Chem. Phys. **122**, 094708 (2005).
[117] C. Herrmann and G. Solomon, ARTAIOS—a transport code for postprocessing quantum chemical electronic structure calculations.
[118] L. Y. Shao, L. Fusti Molna, Y. Jung, J. Kussmann, C. Ochsenfeld, S. T. Brown, A. T. B. Gilbert, L. V. Slipchenko, S. V. Levchenko, D. P. O'Neill, R. A. DiStasio Jr., R. C. Lochan, T. Wang, G. J. O. Beran, N. A. Besley, J. M. Herbert, C. Yeh Lin, T. Van Voorhis, S. Hung Chien, A. Sodt, R. P. Steele, V. A. Rassolov, P. E. Maslen, P. P. Korambath, R. D. Adamson, B. Austin, J. Baker, E. F. C. Byrd, H. Dachsel, R. J. Doerksen, A. Dreuw, B. D. Dunietz, A. D. Dutoi, T. R. Furlani, S. R. Gwaltney, A. Heyden, S. Hirata, C.-P. Hsu, G. Kedziora, R. Z. Khalliulin, P. Klunzinger, A. M. Lee, M. S. Lee, W. Liang, I. Lotan, N. Nair, B. Peters, E. I. Proynov, P. A. Pieniazek, Y. Min Rhee, J. Ritchie, E. Rosta, C. David Sherrill, A. C. Simmonett, J. E. Subotnik, H. Lee Woodcock III, W. Zhang, A. T. Bell, and A. K. Chakraborty, Phys. Chem. Chem. Phys. **8**, 3172 (2006); http://www.q-chem.com.
[119] G. te Velde, F. M. Bickelhaupt, E. J. Baerends, C. Fonseca Guerra, S. J. A. van Gisbergen, J. G. Snijders, and T. J. Ziegler, J. Comput. Chem. **22**, 931 (2001), Amsterdam Density Functional Program; Theoretical Chemistry, Vrije Universiteit Amsterdam; http://www.scm.com.
[120] A. D. Becke, Phys. Rev. A **38**, 3098 (1988).
[121] J. P. Perdew, Phys. Rev. B **33**, 8822 (1986).
[122] P. J. Hay and W. R. Wadt, J. Phys. Chem. **82**, 270 (1985).
[123] A. Schäfer, H. Horn, and R. Ahlrichs, J. Chem. Phys. **97**, 2571 (1992).
[124] A. Schäfer, C. Huber, and R. Ahlrichs, J. Chem. Phys. **100**, 5829 (1994).
[125] D. Andrae, U. Häussermann, M. Dolg, H. Stoll, and H. Preuss, Theor. Chim. Acta **77**, 123 (1990).
[126] N. W. Ashcroft and N. D. Mermin, *Solid State Physics* (Holt, Rinehart and Winston, New York, 1976).